International Journal of Engineering Research and Technology. ISSN 0974-3154, Volume 12, Number 4 (2019), pp. 486-493

Symbols Frequency based Image Coding for Stereoscopic Image

Thafseela Koya Poolakkachalil
PhD Scholar,
National Institute of Technology
Durgapur, India

Saravanan Chandran
Associate Professor,
National Institute of Technology
Durgapur, India

Abstract
The concept behind stereoscopy is that two images that are marginally different are shown separately to the left and right human eyes. The brain combines these images to produce a perception of 3D vision. The storage data or transmission data required for stereoscopic image is twice or even more when compared to two-dimensional (2D) image. Thus, this initiate effective compression technique that reduces the storage requirement and transmission bandwidth required for stereoscopic images. A new compression model *Symbols Frequency based Image Coding for Stereoscopic Image (SFICSI*) is proposed in this article for stereoscopic image compression. In this new model the dissimilarity between left and right images and the left image is encoded separately using Symbols Frequency based Image Coding (SFIC). The decoding of the encoded data results in the synthesis of the retrieved left and right images with high compression ratio while at the same time maintaining the quality of the images. The recommended scheme is also compared with DWT based Arithmetic Coding (DWTAC). From the experimental analysis, it is observed that the proposed new SFICSI outperforms DWTAC.

Keywords: stereoscopic image, image compression, lossless compression, lossy compression

I. INTRODUCTION

Image stereoscopy is a research field that has received great notice recently. The main idea behind stereoscopy is that two images that are marginally different are shown in a particular technique to the human eyes. The brain combines these two images and perceives 3D vision[1]. The principle of stereoscopic work is, manipulating the ability of the Human visual system (HVS) to recognize the difference between two stereo pair images that result in the realization of a perceptual image with depth insight. This is the result of two interactions with respect to binocular vision namely fusion and suppression[2].

The advancements in the field of stereoscopic display and network technologies resulted in the widespread application of 3D image processing technologies in 3D television (3DTV), and Free Viewpoint Video (FVV) [2][3][4][5][6]. Other applications of stereoscopy include stereoscopic video cameras[7], judgement of position and distance, identification of objects, spatial manipulation of objects, navigation, and spatial understanding[8], medicine[9], military[10], industrial computer aided design[11] and photogrammetry[11].

Provision of high quality content is the key factor that indicate the success of 3D applications[12], but at the same time brings in new concerns and challenges[13][14][15]. The storage data and transmission data required for stereoscopic image is twice or even more when compared to two-dimensional (2D) image[16]. As a result, number of image compression systems has been proposed [2][17][18][19]. For the effective transmission of stereo pair images, for the use in 3D systems, compression is adopted before transmission. This initiated for designing efficient coder for the compression of images[20].

The method of reducing the redundant information in an image with the help of various encoding scheme to achieve lesser storage requirement but at the same time does not completely compromise the quality of image is known as image compression. The advantages provided by image compression include lesser transmission time and reduced storage requirement[21][22][23]. There is a recent shift from gray scale image compression related research work to color image compression due to the extensive use of color images in multimedia as well as over internet[24][25][26]. Thus, this research article focuses on color images from LIVE database. The image encoder works well with grayscale images. The spatial redundancy between two images that are marginally different or the stereo pair is exploited to achieve high compression ratio for stereoscopic images[20].

One of the approaches in stereo pair compression focus on disparity compensated residual system where one view acts as a base to predict the another and where coding of their difference takes place[20][27][28][29][30][31][32]. The commonly used approach here was the monoscopic encoding of one channel and then the prediction based encoding of the disparity vector or the residual image[20]. The compression scheme that involves the SFIC encoding of quantized disparity vector and the left image is the focus of this research article.

II. RELATED STEREOSCOPIC IMAGE COMPRESSION WORKS

Che-Chun et al. introduced a new model for stereoscopic images that captures distorted image's spatial correlation[33]. The average Peak Signal to Noise Ratio (PSNR) obtained through this approach was 6.51. This approach motivated to develop a coding scheme for stereo images by avoiding the spatial correlation. Yu-Hsun and Ja-Ling proposed a new metric for stereoscopic image quality analysis[34]. The noticeable improvement is observed in performance even if one stereo image is generated from another stereo image. This initiated motivation to synthesize right image from the retrieved left image.

Ankit et al. compared the approaches for mixed resolution coding for stereo images with reference to their visual fatigue using three methods[35]. It was observed from the results that use cases for each method was directly depended on the time required for viewing, frame rate, and amount of down sampling. This directed to develop a coding scheme that uses a reference image and a disparity vector in the encoding process. Maija et al. developed a new model for stereoscopic image compression on the influence of depth cues as well as compression levels on the quality of the image on as well as depth on an autostereoscopic display[36]. It was observed from the results that the presence of stereoscopic cues helps the visual system in humans to make more reliable depth estimates. This motivated to develop a coding scheme where high compression ratio is attained without compromising the quality of the image.

Feng et al. proposed a new multimodal blind system where the quality valuation of multiply distorted stereoscopic images was completed[37]. The Root Mean Square Error (RMSE) obtained through this approach was 0.0757. This approach initiated to concentrate on a coding scheme where quality of the image is not compromised. Rafik et al. developed a new model for image quality metric where the main idea was the reproduction of the signal produced by the simple and complex cells to calculate the linked binocular energy[38]. The average RMSE achieved through this method was 0.8741. This approach directed to reproduce the images after encoding using a decoder that uses SFIC decoding.

Kaaniche et al. proposed compression scheme for a 2D non-separable stimulating systems that enabled exact decoding and progressive reconstruction of still and stereo images[39]. The advantage was the yielding of attractable optimization of all the intricate decomposition operators. The PSNR obtained through this approach was 30.41 and the average Compression Ratio (CR) was 28.57. This approach motivated to reproduce the stereo pair images with high compression ratio and PSNR.

Balasubramanyam et al. recommended a novel coding scheme for natural stereo images where the algorithm could accurately capture joint statistics of residual sub band coefficients and luminance[40]. The average PSNR obtained through this approach was 41.0466. This approach initiated to develop a novel coding scheme that provides high performance for stereo images. Lijun et al. proposed a coding scheme where the removal of artifacts in depth image is completed by binary segmentation based depth filtering[41]. This directed to develop an encoder that includes compression of depth images in the encoder.

III. RELATED IMAGE COMPRESSION WORKS

Hannuksela et al. proposed a new coding scheme that was compatible with advanced video coding (H.264/AVC) standard and its multiview video coding (MVC) extension[42]. The experimental results produced an average bitrate reduction of 26% and 35% on test scenes. Jiheng et al. proposed a model that helped in the prediction of dissimilar disparities quantitatively for asymmetric video compression[43]. Results showed that this model expected the coding improvement in asymmetric video compression that involves mixed-distortion. The average PSNR achieved through this approach was 11.25.

Tilo Struts proposed a new prediction technique where the image data is treated as interleaved sequence generated by multiple sources[44]. The method achieved lossless color image compression. The average CR obtained through this method was 13.613. Tilo Struts proposed a family of multiplier less transform for color images that was reversible and inspected their performance in lossless image compression[45]. The average CR obtained through this method was 12.48. This approach initiated to include color transforms before encoding.

Che-Chun Su proposed the OCMDNI[33] with Application of a no-reference Natural Stereopair Quality index (S3D-BLINQ Index). OCMDNI achieved high correlations to S3D image quality using the novel bitrate and correlation NSS models. Here an automatic no-reference (NR) S3D image quality model was developed. In this model, it was possible to predict the quality of S3D images, that made it useful for practical applications. Here, 2D IQA algorithm was applied to left and right stereo pair images and the quality of the image was analyzed. The average CR obtained through this method was 1.61.

In 3D-BLINQ Index, a convergent cyclopean was formed for an image using the disparity vector formed by evaluating the left and right images of stereoscopic image. The next stage consisted of extracting the spatial and wavelet domain features and bivariate and correlation NSS features. These features were extracted from the convergent cyclopean image. The mapping of the extracted features to human opinion scores were completed to predict quality S3D image[33]. The PSNR obtained through this approach was 6.51. This research article proposes a new compression technique for stereoscopic images using the left image difference vector. The technique named as Symbols Frequency based Image Coding for Stereoscopic Image (SFICSI) is analyses for Color Image Compression. The following section IV explains the proposed new SFICSI technique. The section V discusses about the experiments and results, analyses SFICSI and compares with DWTAC. Conclusions are drawn in section VI.

IV. STEREOSCOPIC IMAGE COMPRESSION

Two main factors that indicate the performance of an encoder are Compression Ratio (CR) and Peak Signal to Noise ratio (PSNR). CR gives clue of the rate of compression. PSNR is an indication of the quality of the reconstructed image after decoding.

a) Compression Ratio

The ratio of added size of the original left image and right image (l+r) and the added size of the compressed image (cl+cr) [49].

$$CR=(l+r)/(cl+cr) \tag{1}$$

b) Peak Signal to Noise Ratio

PSNR is an expression for the ratio between the maximum possible value (power) of a signal and the power of distorting noise that affects the quality of its representation[26].

The mathematical representation of the PSNR is as follows:

$$PSNR = 20\log_{10}\left(\frac{MAX_f}{\sqrt{MSE}}\right) \quad (2)$$

where, *MSE* (Mean Square Error) is the error factor. *MSEL* and *MSER* is initially calculated using Equation (3) and is fed into Equation to generate PSNRL and PSNRR (2).

$$MSE = \frac{1}{mn}\sum_{0}^{m-1}\sum_{0}^{n-1}\|f(i,j) - g(i,j)\|^2 \quad (3)$$

Quantization process in the image compression technique results in the scaling of the data set by quantization factor that results in data loss that is irreversible and the respective encoding process becomes lossy compression[25].

A. Proposed new SFICSI Scheme

In this section, the new compression scheme for stereoscopic images namely, SFICSI, is explained, where SFIC[25] is used as the encoder. The flowchart of SFICSI is displayed in figure 1 while the flowchart of SFIC is displayed in figure 2.

In the initial stage of SFICSI, the transformed matrix of the left and right stereoscopic image is retrieved. Further, colour components of the stereoscopic left image and right image are extracted. In the next step quantization of the colour components of the transformed matrices is completed. Further the encoding scheme is completed using SFIC encoding[25] for the disparity vector, D, obtained by mapping the dissimilarity between left and right image, and the left image L. CR is calculated from the results of encoding using equation 1.

During the encoding process, separate symbol tables are generated for L and D. A sample symbol table is shown in the following table I. The symbol table consists of pixel values(symb), frequency of symbols(count), and index of the pixels(index) in L and D. In the symbol table, first column represents the unique elements, second column represents the frequency of symbols, and third column represents the index assigned to each of the unique elements. The input for the encoder is the index_matrix_o that contains the quantized L and D values rewritten in terms of index assigned in the symbol table. In the next stage, minimal frequency symbol matrix is generated.

An illustration of the methodology is explained below. For example, part of the source left image matrix is considered as L and part of source right image is considered as R.

L =

107	114	125	124	121
105	95	101	102	104
101	106	105	107	104
107	107	98	84	110
96	63	62	61	62

R=

85	92	101	115	115
115	93	99	99	99
97	95	101	99	100
102	99	100	92	85
92	83	85	84	89

The following CL and CR represents the colour space transformed Y components of above L and R respectively. For illustrative purpose, one of the colour space components of L and R are shown below.

CL=

83.2493	89.8631	101.1162	99.6554	97.1768
80.4254	67.1334	70.3824	70.6391	70.5507
68.5763	73.9765	73.8177	74.2333	69.9487
74.0375	74.6395	68.9121	60.2903	85.9236
73.9001	45.4610	44.6022	44.3454	44.6022

CR=

65.0551	71.1647	80.0003	92.0239	92.0239
90.7219	65.6116	67.4606	68.7626	68.3564
65.8409	65.9294	71.5864	66.4524	66.6113
68.8330	68.0627	71.1338	64.7528	60.6450
67.3567	57.6254	59.3430	59.0863	63.3804

The following D represents the disparity vector obtained from CL and CR

D=

18.1942	18.6983	21.1159	7.6315	5.1529
-10.2964	1.5218	2.9217	1.8765	2.1943
2.7354	8.0472	2.2312	7.7809	3.3374
5.2045	6.5769	-2.2218	-4.4624	25.2786
6.5434	-12.1644	-14.7408	-14.7408	-18.7782

In the next stage, quantization is applied to CL and D. The following QCL represents the quantized CL values.

QCL=

84	92	100	100	100
84	68	68	68	68
76	84	100	100	100
84	68	76	76	68
68	76	84	100	92

The quantized D data, QD is generated in the same method. Further, SFIC encoding is applied to CL and D and the encoded data is obtained. In order to accomplish this, separate symbol table with the unique pixel value, frequency of occurrences, and an index are generated for CL and D. The following table I shows the symbol table of QCL, namely TABQCL. In the symbol table TABQCL, first column represents the unique elements (symb), second column the frequency of occurrence (count), and third column represents the index assigned to each of symb (index).

Table I Symbol table (TAQCL) of QCL

symb	count	index
68	7	1
76	4	2
84	5	3
92	2	4
100	7	5

In the next stage, index matrix, IQCL is generated using symb and index. IQCL replaces the respective symb in QCL with index values.

IQCL =

3	4	5	5	5
3	1	1	1	1
2	3	5	5	5
3	1	2	2	1
1	2	3	5	4

In the next stage, SFIC encoding is applied to ICL and encoded data, SCL is generated. During decompression, SFIC decoding is applied to the encoded data, RCL, and disparity vector, RD is retrieved. Here, RCL is the retrieved colour transformed left image data. Following is an illustration of RCL and RD.

RCL=

84	76	68	68	68
76	76	76	76	76
92	84	76	68	68
76	76	76	76	68
100	100	84	76	76

RD=

20	20	12	4	4
4	4	4	4	12
20	20	20	4	4
4	4	4	4	4
20	28	20	12	4

Retrieved colour transformed right image data, RCR is obtained by the summation of RCL and RD. The following RCR represents the summated result of RCL and RD.

RCR=

104	96	80	72	72
80	80	80	80	88
112	104	96	72	72
80	80	80	80	72
20	128	104	88	80

In the next stage, inverse colour transform is applied to RCL and RCR. The following RL and RR represents the retrieved left image and retrieved right image obtained after application of inverse colour transform.

RL=

103	112	126	124	121
101	88	96	97	100
96	102	101	103	100
103	103	92	75	107
90	49	47	46	47

RR=

117	126	143	124	121
101	88	96	97	100
96	102	101	103	100
103	103	92	75	126
90	59	63	62	70

Following is the SFICSI encoding algorithm.

SFICSI Encoding Algorithm

1. *Read the source image, L*
2. *Read the frequency factor, y*
3. *Perform the colour space conversion on L*
4. *Generate the symbol table*
5. *Generate indexed data*
6. *Generate the minimal data*
7. *Generate the disparity data*
8. *Generate the unique data*
9. *Compression ratio is calculated*

Encoding algorithm helps in the generation of minimal frequency symbols. A user defined input y is used to find the minimal pixelvalue among y elements in the matrix. In the next stage, index_matrix_m is generated by assigning the minimal value for the y consecutive elements in index_matrix_o. In the next step, index_Diff1 is generated by finding the difference between index_matrix_m and index_matrix_o. In the next step, individual distinct values of index_matrix_m are generated and thus the compressed matrix, index_DataComp is generated. Since a unique element is assigned for every y minimal elements, the resultant index_DataComp generated is highly compressed.

The following figure 1 shows flowchart of SFICSI compression scheme.

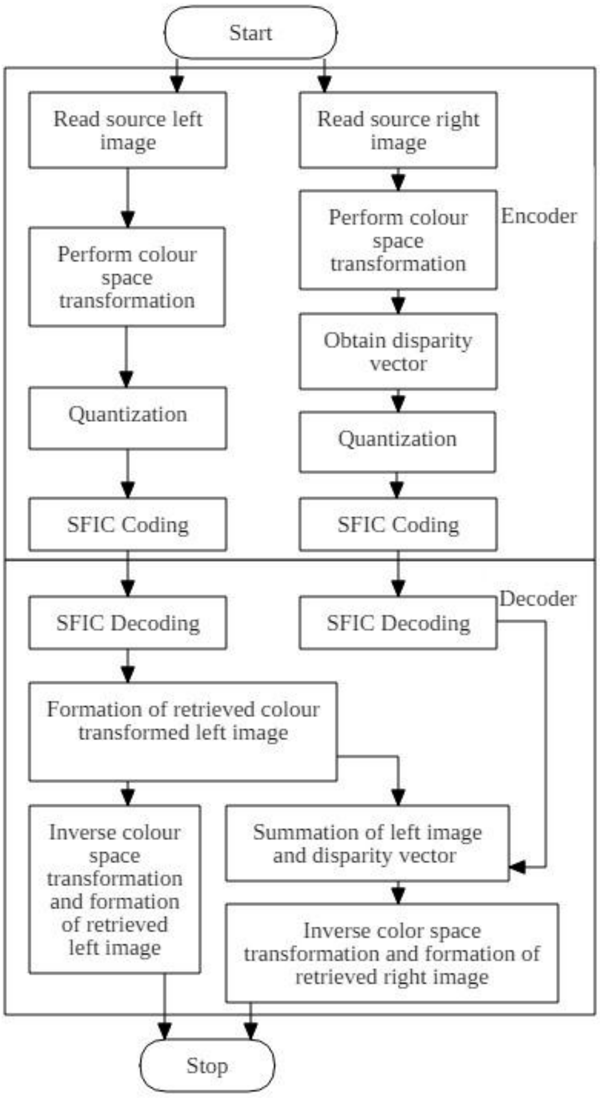

Fig.1 Flowchart of proposed SFICSI

For the reconstruction purpose, transmission of compressed matrix; index_DataComp, frequency factor; y, index_Diff1 and unique symbols will be sufficient. The decoding process is summarized as below.

The following figure 2 shows flowchart of SFIC compression scheme.

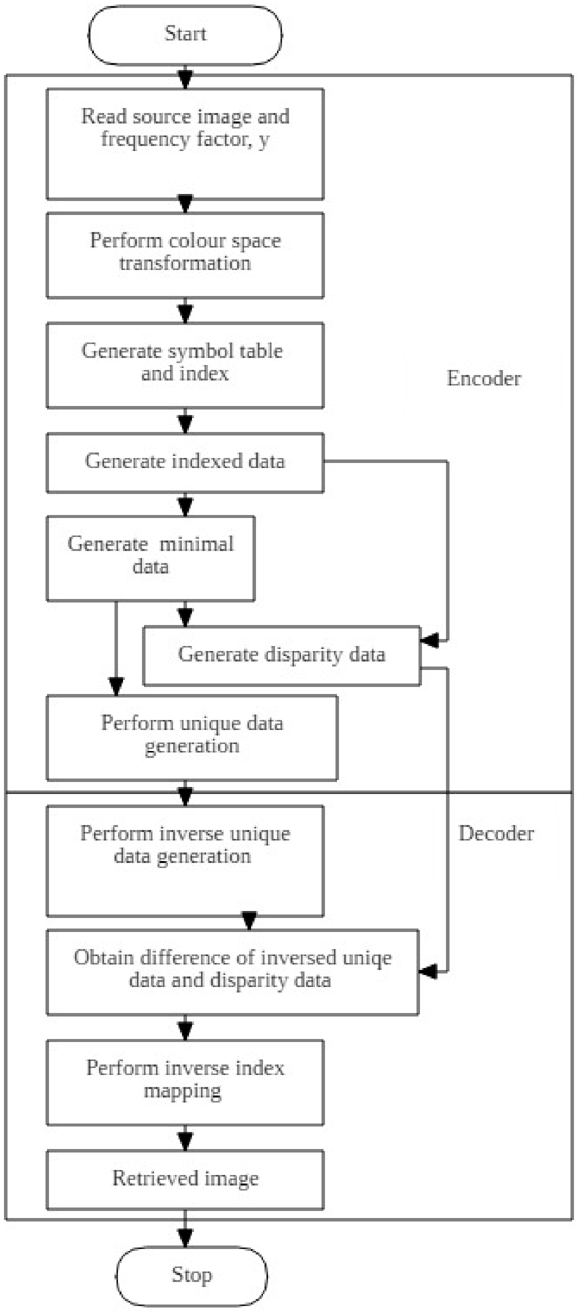

Fig.2 Flowchart of SFIC

International Journal of Engineering Research and Technology. ISSN 0974-3154, Volume 12, Number 4 (2019), pp. 486-493

Following is the SFICSI decoding algorithm.

SFICSI Decoding Algorithm

1. *Read the compressed data*
2. *Read the disparity data*
3. *Perform inverse unique data generation*
4. *Generate the minimal retrieved data*
5. *retrieved indexed data= minimal retrieved data - disparity data*
6. *Perform inverse index mapping*
7. *Perform inverse colour space transformation*
8. *Reproduced image is generated*
9. *PSNR is calculated*

Decoding phase consists of two main stages. In the first step, index_DataRet1 is generated by recursively printing the individual elements in index_DataComp y times. This process regenerates the retrieved index_matrix_m. In the next phase, index_DataRet2 is generated by finding the difference between index_DataRet1 and index_Diff1. This process regenerates the retrieved index_matrix_o. The next phase of SFIC consists of generating the retrieved data, matrix_m by comparing the index_DataRet2 and the unique symbols with respect to index. Index is the number 1 to N assigned in ascending order for the unique symbols.

In the case of SFICSI, matrix_m_l is generated for retrieving left image and matrix_m_d is generated for retrieving disparity vector using SFIC decoding algorithm.

In the next stage, matrix_m_l and matrix_m_d is concatenated to generate matrix_m_r. Inverse colour transform is then applied on matrix_m_l to generate the retrieved left image, RL. Inverse colour transform is applied on matrix_m_l to generate the retrieved right image, RR. From the retrieved left image, RL and the retrieved right image, RR, PSNR is calculated using Equation 2. The following figure 2 shows flowchart of SFIC compression scheme.

V. RESULTS

The following table I shows the Compression Ratio (CR) and PSNR for the images used for testing using the proposed new SFICSI compression scheme for images.

Table I. Compression Ratio and PSNR using the proposed SFICSI

Source Images	CR	PSNR	
	SFICSI	Left Image	Right Image
im3	12.9474	44.6377	41.6008
im5	9.9388	35.3094	35.8395
im10	12.0750	37.0683	31.5627
im12	15.2976	41.1002	42.9053
im13	16.3000	48.6570	31.5627

Table II contains the original images used for testing and the reproduced images. The experimental research work and analysis are performed on the standard LIVE 3D image database [52]. It is observed from the results that the highest CR is for im13 (16.3000). The lowest CR is for im5, (9.9388). The highest PSNR of left and right images is 48 and lowest PSNR is 31. However, left images achieved higher PSNR values compared with the right images.

SFICSI is analyzed with a set of color images shown in following table II.

Table II. Source images and reproduced images

Source Image		Reproduced Images	
Left Image	Right Image	Right Image	Right Image
im3_l	im3_l	rim3_l	rim3_r
			
im5_l	im5_l	rim5_l	rim5_r
			
im10_l	im10_l	rim10_l	rim10_r
			
im12_l	im12_l	rim12_l	rim12_r
			
im13_l	im13_l	rim13_l	rim13_r
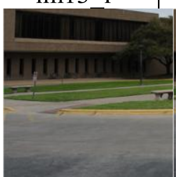			

The following table III shows the comparison results of compression ratios of proposed new SFICSI image compression scheme and DWT based Arithmetic Coding (DWTAC).

Table III. Comparison of CR of SFICSI and DWTAC

Source Images	CR	
	DWTAC	SFICSI
im3	5.7781	12.9474
im5	5.9705	9.9388
im10	4.6689	12.0750
im12	8.2080	15.2976
im13	8.3092	16.3000

The following table IV shows the comparison of PSNR values of proposed new SFICSI image compression scheme and DWT based Arithmetic Coding (DWTAC).

Table IV. Comparison of PSNR of SFICSI and DWTAC

Source Images	PSNR DWTAC		PSNR SFICSI	
	Left Image	Right Image	Left Image	Right Image
im3	41.9888	44.6377	44.6377	41.6008
im5	29.3674	35.3094	35.3094	35.8395
im10	32.9700	37.0683	37.0683	31.5627
im12	33.0860	41.1002	41.1002	42.9053
im13	39.9287	48.6570	48.6570	31.5627

In the above table III and table IV, SFICSI is compared with DWTAC. It is observed from the experimental analysis that the proposed new SFICSI coding achieves better compression ratio 6 - 11 % improvement compared with DWTAC. It is also observed that the proposed SFICSI achieved higher PSNR values compared with DWTAC. Thus, SFICSI outperforms DWTAC.

VI. CONCLUSION

A new approach for stereoscopic image compression is proposed in this research article. In this new approach, SFIC encoding algorithm is applied on left image and disparity vector mapping between images. It is observed from the experimental analysis that the proposed SFICSI scheme exhibits higher compression ratio and higher PSNR values. This new compression method is compared with DWT based Arithmetic Coding (DWTAC). It is observed that SFICSI outperforms DWTAC.

REFERENCES

[1] S. Ouddane, K. M. Faraoun, S. A. Fezza, and M. C. Larabi, "Adaptive colorization-based compression for stereoscopic images," *3DTV-Conference*, vol. 2016–Augus, pp. 3–6, 2016.

[2] G. Jiang, J. Zhou, M. Yu, Y. Zhang, F. Shao, and Z. Peng, "Binocular vision based objective quality assessment method for stereoscopic images," *Multimed. Tools Appl.*, vol. 74, no. 18, pp. 8197–8218, 2015.

[3] J. Lee, K. Yun, and K. Kim, "A 3DTV broadcasting scheme for high-quality stereoscopic content over a hybrid network," *IEEE Trans. Broadcast.*, vol. 59, no. 2, pp. 281–289, 2013.

[4] S. Zinger, L. Do, and P. H. N. de With, "Recent developments in free-viewpoint interpolation for 3DTV," *3D Res.*, vol. 3, no. 1, pp. 1–6, 2012.

[5] Y. C. Fan, Y. T. Kung, and B. L. Lin, "Three-dimensional auto-stereoscopic image recording, mapping and synthesis system for multiview 3D display," in *IEEE Transactions on Magnetics*, 2011, vol. 47, no. 3, pp. 683–686.

[6] H. Urey, K. V. Chellappan, E. Erden, and P. Surman, "State of the art in stereoscopic and autostereoscopic displays," in *Proceedings of the IEEE*, 2011, vol. 99, no. 4, pp. 540–555.

[7] Mendiburu ; Bernard, *3D TV and 3D Cinema: Tools and Processes for Creative Stereoscopy1. Mendiburu ; Bernard. 3D TV and 3D Cinema: Tools and Processes for Creative Stereoscopy. Focal Press; 2011.* Focal Press, 2011.

[8] J. P. McIntire, P. R. Havig, and E. E. Geiselman, "What is 3D good for? A review of human performance on stereoscopic 3D displays," *SPIE defense, Secur. sensing. Int. Soc. Opt. Photonics.*, p. 83830X–83830X, 2012.

[9] D. J. Getty and P. J. Green, "Clinical applications for stereoscopic 3-D displays," *J. Soc. Inf. Disp.*, vol. 15, no. 6, p. 377, 2007.

[10] S. Dixon, E. Fitzhugh, and D. Aleva, "Human factors guidelines for applications of 3D perspectives: a literature review," vol. 7327, p. 73270K, 2009.

[11] J. J. Gallimore, "Visualization of Three-Dimensional Structure During Computer-Aided Design," *Int. J. Hum. Comput. Interact.*, vol. 7, no. 1, pp. 37–56, 1995.

[12] S. Mahmoudpour and M. Kim, "The effect of depth map up-sampling on the overall quality of stereopairs," *Displays*, vol. 43, pp. 9–17, 2016.

[13] X. Li, Q. Ruan, Y. Jin, G. An, and R. Zhao, "Fully automatic 3D facial expression recognition using polytypic multi-block local binary patterns," *Signal Processing*, vol. 108, pp. 297–308, 2015.

[14] A. Vosoughi, V. Testoni, P. C. Cosman, and L. B. Milstein, "Multiview coding and error correction coding for 3D video over noisy channels," *Signal Process. Image Commun.*, vol. 30, pp. 107–120, 2015.

[15] Y. Liu, J. Yang, and R. Chu, "Objective evaluation criteria for shooting quality of stereo cameras over short distance," *Radioengineering*, vol. 24, no. 1, pp. 305–313, 2015.

[16] A. Vetro, A. M. Tourapis, K. Müller, and T. Chen, "3D-TV content storage and transmission," *IEEE Trans. Broadcast.*, vol. 57, no. 2 PART 2, pp. 384–394, 2011.

[17] M. Dománski *et al.*, "High efficiency 3D video coding using new tools based on view synthesis.," *IEEE Trans. Image Process.*, vol. 22, no. 9, pp. 3517–3527, 2013.

[18] M. K. Kang, C. Lee, J. Y. Lee, and Y. S. Ho, "Adaptive geometry-based intra prediction for depth video coding," in *2010 IEEE International Conference on Multimedia and Expo, ICME 2010*, 2010, pp. 1230–1235.

[19] F. Shao, G. Jiang, W. Lin, M. Yu, and Q. Dai, "Joint bit allocation and rate control for coding multi-view video plus depth based 3D video," *IEEE Trans. Multimed.*, vol. 15, no. 8, pp. 1843–1854, 2013.

[20] W. Yuanqing, "Estimating the minimum redundancy in stereo image pair," *Image Vis. Comput.*, vol. 26, no. 5, pp. 725–730, 2008.

[21] K. L. Chung, H. L. Huang, and H. I. Lu, "Efficient region segmentation on compressed gray images using quadtree and shading representation," *Pattern Recognit.*, vol. 37, no. 8, pp. 1591–1605, 2004.

[22] G. Zhai, W. Lin, J. Cai, X. Yang, and W. Zhang, "Efficient quadtree based block-shift filtering for deblocking and deringing," *J. Vis. Commun. Image Represent.*, vol. 20, no. 8, pp. 595–607, 2009.

[23] T. K. Poolakkachalil, S. Chandran, and K. Vijayalakshmi, "Analysis of application of arithmetic coding on dct and dct-dwt hybrid transforms of images for compression," in *2017 International Conference on Networks and Advances in Computational Technologies, NetACT 2017*, 2017.

[24] W.-L. Chen, Y.-C. Hu, K.-Y. Liu, C.-C. Lo, and C.-H. Wen, "Variable-Rate Quadtree-segmented Block Truncation Coding for Color Image Compression," *Int. J. Signal Process. Image Process. Pattern Recognit.*, vol. 7, no. 1, pp. 65–76, 2014.

[25] P. G. K. Kharate, "Color Image Compression Based On Wavelet Packet Best Tree," vol. 7, no. 2, pp. 31–35, 2010.

[26] T. Koya Poolakkachalil and S. Chandran, "Symbols Frequency based Image Coding for Compression," vol. 15, no. 9, pp. 148–155, 2017.

[27] M. Siegel, P. Gunatilake, S. Sethuraman, and A. Jordan, "Compression of stereo image pairs and streams," in *Stereoscopic Displays and Virtual Reality Systems. SPIE*, 1994, pp. 258–268.

[28] K. Zeger, "Residual image coding for stereo image compression," *Opt. Eng.*, vol. 2, no. 1, p. 182, 2003.

[29] R. Hawkins, "Digital Stereo Video: display, compression and transmission," no. February, pp. 1–148, 2002.

[30] M. S. Moellenhoff and M. W. Maier, "Transform coding of stereo image residuals," *IEEE Trans. Image Process.*, vol. 7, no. 6, pp. 804–812, 1998.

[31] J. Konrad and Z. D. Lan, "Dense disparity estimation from feature correspondences," *{Proc} {Spie} {Int} {Soc} {Opt} {Eng}*, vol. 3957, pp. 90–101, 2000.

[32] M. Siegel, S. Sethuraman, J. S. McVeigh, and A. Jordan, "Compression and Interpolation of {3D}-Stereoscopic and Multi-View Video," *SPIE Stereosc. Disp. Virtual Real. Syst. IV*, vol. 3012, pp. 227–238, 1997.

[33] C. C. Su, L. K. Cormack, and A. C. Bovik, "Oriented Correlation Models of Distorted Natural Images With Application to Natural Stereopair Quality Evaluation," *IEEE Trans. Image Process.*, vol. 24, no. 5, pp. 1685–1699, 2015.

[34] Y. H. Lin and J. L. Wu, "Quality assessment of stereoscopic 3d image compression by binocular integration behaviors," *IEEE Trans. Image Process.*, vol. 23, no. 4, pp. 1527–1542, 2014.

[35] A. K. Jain, A. E. Robinson, and T. Q. Nguyen, "Comparing perceived quality and fatigue for two methods of mixed resolution stereoscopic coding," *IEEE Trans. Circuits Syst. Video Technol.*, vol. 24, no. 3, pp. 418–429, 2014.

[36] M. Mikkola, S. Jumisko-Pyykko, D. Strohmeier, A. Boev, and A. Gotchev, "Stereoscopic depth cues outperform monocular ones on autostereoscopic display," *IEEE J. Sel. Top. Signal Process.*, vol. 6, no. 6, pp. 698–709, 2012.

[37] F. Shao, W. Tian, W. Lin, G. Jiang, and Q. Dai, "Learning sparse representation for no-reference quality assessment of multiply-distorted stereoscopic images," *IEEE Trans. Multimed.*, vol. 9210, no. c, pp. 1–1, 2017.

[38] R. Bensalma and M. C. Larabi, "A perceptual metric for stereoscopic image quality assessment based on the binocular energy," *Multidimens. Syst. Signal Process.*, vol. 24, no. 2, pp. 281–316, 2013.

[39] M. Kaaniche, A. Benazza-Benyahia, B. Pesquet-Popescu, and J. C. Pesquet, "Non-separable lifting scheme with adaptive update step for still and stereo image coding," *Signal Processing*, vol. 91, no. 12, pp. 2767–2782, 2011.

[40] B. Appina, S. Khan, and S. S. Channappayya, "No-reference Stereoscopic Image Quality Assessment Using Natural Scene Statistics," *Signal Process. Image Commun.*, vol. 43, pp. 1–14, 2016.

[41] L. Zhao, H. Bai, A. Wang, Y. Zhao, and B. Zeng, "Signal Processing : Image Communication Two-stage fi ltering of compressed depth images with Markov Random Field," *Signal Process. Image Commun.*, vol. 54, no. September 2016, pp. 11–22, 2017.

[42] M. M. Hannuksela *et al.*, "Multiview-video-plus-depth Coding based on the Advanced Video Coding Standard," *IEEE Trans. Image Process.*, vol. 22, no. 9, pp. 3449–58, 2013.

[43] J. Wang, S. Wang, and Z. Wang, "Asymmetrically Compressed Stereoscopic 3D Videos: Quality Assessment and Rate-Distortion Performance Evaluation," in *IEEE Transactions on Image Processing*, 2017, vol. 26, no. 3, pp. 1330–1343.

[44] T. Strutz, "Context-Based Predictor Blending for Lossless Color Image Compression," *IEEE Trans. Circuits Syst. Video Technol.*, vol. 26, no. 4, pp. 687–695, 2016.

[45] T. Strutz, "Multiplierless reversible color transforms and their automatic selection for image data compression," *IEEE Trans. Circuits Syst. Video Technol.*, vol. 23, no. 7, pp. 1249–1259, 2013.